

# Measuring the Speed of Light Using a Helium Neon Laser

Caitlyn Kloeckl  
December 20th, 2020

## Abstract

The goal of the experiment was to measure the speed of light using a helium neon laser. By varying the laser cavity length, various frequencies were produced in the laser cavity. The various frequencies interfered and produced a beat frequency which was measured. Plotting the beat frequency against the cavity length produced a linear fit, and the speed of light was determined from the slope of that line. The value for the speed of light in air was measured to be  $(3.0019 \pm 0.0034) * 10^8 \text{ m/s}$ .

## Introduction

The speed of light has been known to within 5% since the late 17th century,<sup>1</sup> and the measurement has steadily improved until the 1983 redefinition of the meter in terms of the speed of light.<sup>2</sup> At the time of the first measurement, the speed of light was a mere curiosity, since there were no instruments or techniques which could conduct the measurements. However, since then new physics and technology have been developed which depend on the precise value of the speed of light. Many laboratory techniques, such as interferometry, energy measurements, and long-distance measurements, depend on knowing precisely how fast light travels, both in vacuum and in air.

With the advent of the laser, which produces coherent, nearly monochromatic light, novel methods for the measurement of the speed of light have become available. One such method

involves measuring the length of a laser cavity and observing the difference between the frequencies of the standing waves within the laser cavity. The measurement was first performed in 1979, and the researchers<sup>3</sup> found the speed of light to be  $3.053 \pm 0.063 \times 10^8$  m/s. This experiment sought to improve the measurement by using more advanced techniques than were available at the time, and by varying the length of the laser cavity and using statistical techniques to reduce uncertainty. Our method has been successfully deployed<sup>4</sup> in recent years and measured the speed of light in air as  $2.9972 \pm 0.0002 \times 10^8$  m/s.

The following experiment has replicated similar results using an open-cavity helium-neon laser. The cavity length was varied, the intensity of the beam using a photodetector was measured, and a spectrum analyzer was used to determine the beat frequency. A linear fit yielded the speed of light.

## Theory

A laser creates a standing electromagnetic wave in a cavity containing a gain medium. The medium for the laser used in this experiment is a mixture of helium and neon gas. When voltage is applied across the tube, a discharge arc excites the atoms within the tube. Most of these atoms rapidly decay by emitting photons, however some of the excited states in the helium atoms are metastable.<sup>5</sup> These metastable helium atoms survive long enough to collide with other atoms.

Since there are excited states in neon with energies near to those of metastable helium, a collision between a metastable helium atom and a low-energy neon atom can cause the neon atom to enter the excited state.<sup>5</sup> Since there are many more helium atoms than neon atoms, this can cause most of the neon atoms to be excited. This state is known as population inversion.

Some of the excited neon atoms release a photon and decay to a low-energy state, in a process known as spontaneous emission. Spontaneous emission takes place randomly and produces incoherent light. Other excited atoms experience stimulated emission, where a photon emitted spontaneously interacts with another excited atom and triggers its decay.<sup>5</sup> The interaction causes the excited atom to emit a photon with the same wavelength, phase, and direction as the triggering photon. This produces coherent light in the laser cavity. The curved mirrors at both ends of the cavity ensure that some of the light is retained. While the cavity length is less than the radius of curvature of either mirror (or between the radii of curvature of both mirrors), the mirrors focus the light into the cavity, creating a standing wave. In a population inversion, the excited state is more common than the ground state, so stimulated emission becomes more frequent as the wave amplitude increases.

Elementary statistical mechanics tell us these neon atoms are moving at 600 m/s at room temperature. Since the direction of motion is random, the component of the velocity directed along the cavity is also random. This means an emitted photon has a random initial velocity. So, the photons emitted are Doppler-shifted by a random amount. The doppler shift causes changes in wavelength, as depicted in Figure 1. Because of the doppler shift, the light in the cavity varies in wavelength. This phenomenon is called Doppler broadening and is a critical phenomenon which was manipulated in the experiment.

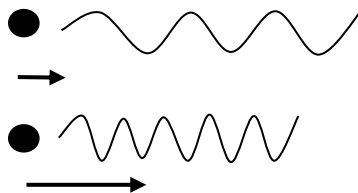


Figure 1. The doppler effect on a photon emitted with low velocity (top) and one emitted with higher velocity (bottom).

Once emitted, the photons pass through a laser cavity with mirrors at both ends. The mirrors apply a boundary condition on the standing wave that forces the electric field to be zero at both ends of the cavity. So, only a certain set of discrete frequencies are permitted in the cavity.

A naïve analysis would show an integer number of half-wavelengths filling the distance between the two mirrors. However, the laser cavity is not uniform. Figure 2 shows that each region of the laser cavity has a particular index of refraction  $n$  and length  $L$ .

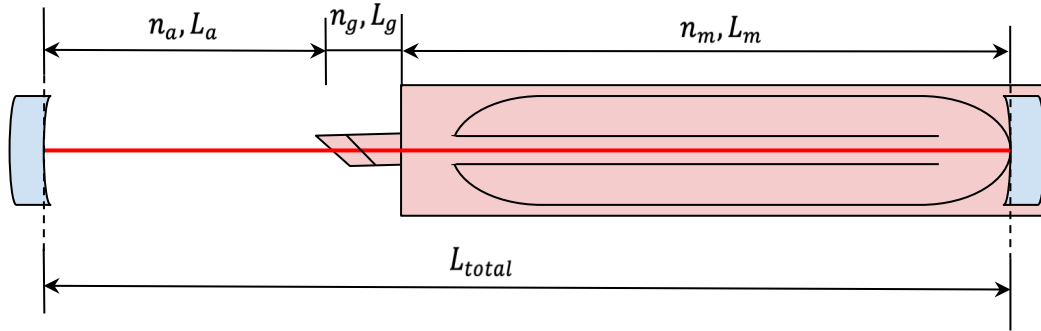


Figure 2: The laser, with lengths and respective refractive indices of the various sections.  $n_a$  is the refractive index of air,  $n_g$  is the refractive index of glass, and  $n_m$  is the refractive index of the laser medium, the helium-neon gas. Similarly, each  $L_i$  is the length of the respective section.

Since light travels with speed  $v = \frac{c}{n}$  in a medium with index of refraction  $n$ , the wavelength is different in each region of the tube. Therefore, to determine the modified length of the cavity as a multiple of the vacuum wavelength  $\lambda$ , each portion of the cavity is separated. The wavelength in glass is  $\frac{\lambda}{n_g}$ , so the laser spends  $\frac{2L_g n_g}{\lambda}$  wavelengths there. The case for air and the gain medium are similar, so the cavity contains  $N = \frac{2(L_g n_g + L_a n_a + L_m n_m)}{\lambda}$  wavelengths of the laser light. For the constructive interference critical to lasing,  $2N$  must be an integer. Therefore, only frequencies for which the half-wavelength evenly divides the cavity length are permitted.

After passing through the cavity, the discrete set of permitted frequencies appear with a Gaussian gain profile centered at the optimal wavelength for the laser (see Fig. 3). Here, that optimal wavelength is 632.8 nm. Because the series of delta functions corresponding to the permitted wavelengths is present with the Gaussian corresponding to the emitted wavelengths, there are several (usually two or three, since the width of this Gaussian is about three times the separation of the delta functions) peaks which are significantly higher than the rest.

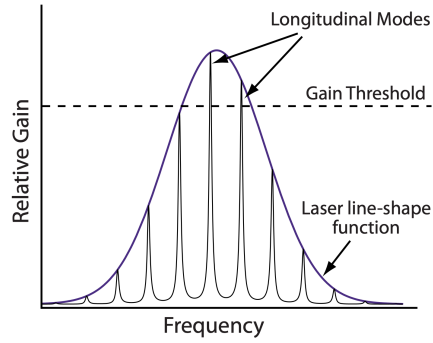


Figure 3: Longitudinal cavity modes on a Gaussian gain profile. Image from [3].

When multiple modes are present, interference between them causes the beam intensity to vary in time. The frequency of the intensity changes the beat frequency, and it is equal to the differences between the frequencies of the longitudinal modes labeled in Figure 3. Thus, showing that the beat frequency depends on the length of the cavity and the speed of light.

Consider two adjacent modes, one with  $2N = k$  and vacuum wavelength  $\lambda_k$ , and one with  $2N = k + 1$  and wavelength  $\lambda_{k+1}$ . Then  $k = \frac{2(L_g n_g + L_a n_a + L_m n_m)}{\lambda_k}$  and  $k + 1 = \frac{2(L_g n_g + L_a n_a + L_m n_m)}{\lambda_{k+1}}$ . Rewritten in terms of the frequencies  $f_k$  and  $f_{k+1}$  and subtracting the two equations yields

$$1 = \frac{2(L_g n_g + L_a n_a + L_m n_m)}{c} (f_{k+1} - f_k).$$

Note that the difference  $(f_{k+1} - f_k)$  is exactly the beat frequency  $f_b$ , resulting in

$$\frac{1}{f_b} = \frac{2(L_g n_g + L_m n_m + L_a n_a)}{c}$$

Next, taking  $L_a$  to be some base length  $L_0$  plus some varying length  $\Delta L$ , which gives

$$\frac{1}{f_b} = \frac{2(L_g n_g + L_m n_m + L_0 n_a) + 2\Delta L n_a}{c}$$

Since  $v_a = \frac{c}{n_a}$  is the speed of light in air, this yields:

$$\frac{1}{f_b} = \frac{2(L_g n_g + L_m n_m + L_0 n_a)}{c} + \frac{2\Delta L}{v_a}$$

This produces a linear model for the reciprocal beat frequencies  $\frac{1}{f_b}$  as a function of the cavity

length in air  $\Delta L$ , with slope,  $m$ , corresponding to:

$$m = 2/v_a$$

Unfortunately, this laser mode is not the only possible standing wave. There are two more sets of solutions which satisfy the boundary conditions, higher-order transverse modes given by the Laguerre and Hermite polynomials. Throughout the derivation, it has been assumed the laser operates in the fundamental TEM-00 mode. The higher-order transverse modes have a wider beam and different frequencies than the TEM-00 mode.<sup>6</sup> Due to their different frequencies, they interfere with each other (and the TEM-00 mode) to produce beat frequencies not predicted by this model. However, since the beam is wider in these other modes, these can be excluded from the cavity with an iris: The photons corresponding to the problematic modes are absorbed by the partly closed iris, while the desirable TEM-00 mode fits through the open center.

Since the beat frequency is the primary measured variable, it is critical to minimize the uncertainty. Two problematic phenomena in the laser are frequency pushing and pulling.

Frequency pushing occurs when the varying intensity in the laser cavity causes the index of refraction of the medium to change, causing the effective length (and therefore beat frequency)

to change. To mitigate pushing, measurements must be taken when the laser operates at a consistent intensity.

Frequency pulling occurs because the dependence of the index of refraction on frequency (the dispersion relation) behaves anomalously near the resonance peak of the gain medium. This causes the frequencies of the standing waves to be closer to the resonance frequency of the laser than this model predicts.<sup>7</sup> These problematic effects can be minimized by using the Fabry-Pérot interferometer as detailed below, and by ensuring beat frequency measurements are taken when the two modes are at the same intensity, which should be uniform across cavity lengths.

## Experimental Setup

An open-cavity helium-neon laser was constructed and was operating at 632 nm. The laser tube was mounted to the optics table, and an output coupler was placed on a programmable translation stage mounted to the table. The stepper motor allows fine control of the cavity length. Mirrors directed the beam onto a photodetector, which measured the intensity of the beam. The output of the photodetector was connected to the spectrum analyzer, which isolated the frequency at which the laser's intensity changes.

To minimize frequency pushing and pulling, the intensities of the two frequency modes were ensured to be approximately the same. Ensuring the intensities were approximately the same was done by varying the size of the iris located in the laser cavity, which measured the two intensities using a scanning Fabry-Pérot interferometer that was connected to an oscilloscope. Then, a beam splitter diverted a portion of the laser beam to the interferometer while the beat

frequency was simultaneously measured with the photodetector. A schematic of the apparatus is given in Figure 4 below.

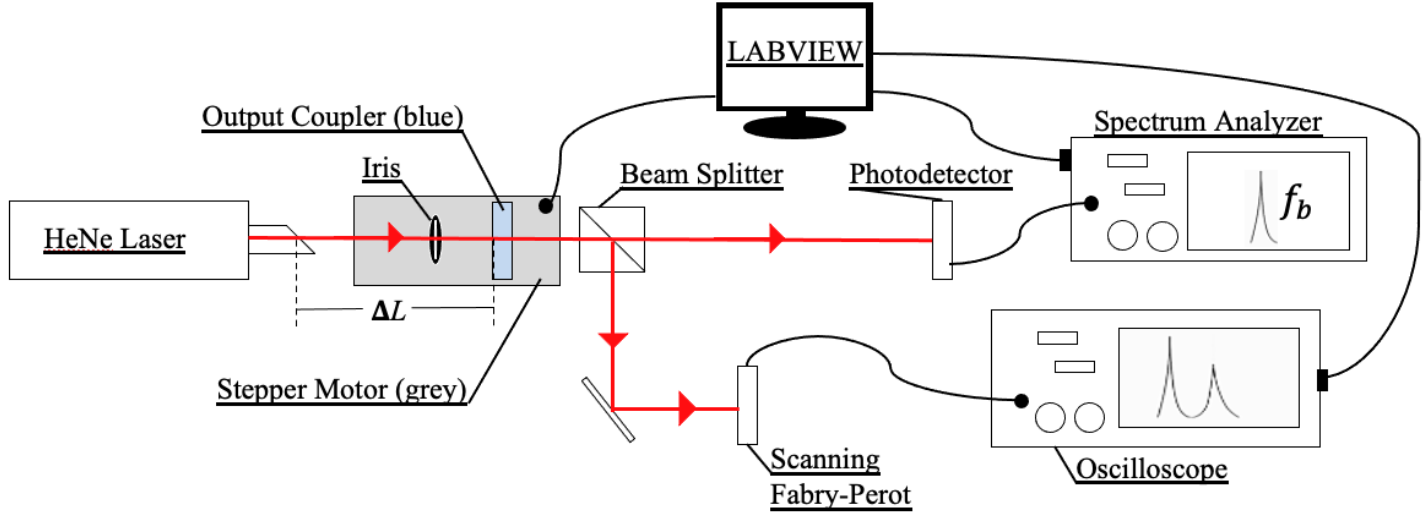


Figure 4: A schematic of the apparatus. The red line represents the path of the laser. The main measured variables are labeled as  $\Delta L$  and  $f_b$  at their relevant locations. The laser cavity is shown in more detail in Figure 2.

The laser tube is a Melles Griot 05-LHB-568, and it was powered with a Melles Griot 05-LHB-568 power supply. The translation stage was manufactured by Micro-Controle, a model number is not available. The stepper motor is a Vexta PK266M-E2.0A and moves at 400 steps per revolution. The photodetector is a Thorlabs RDA8A, connected to a matching power supply and a Rigol DSA815 spectrum analyzer. The scanning Fabry-Pérot interferometer is a Tropel model 7600 with a free spectral range of 7.5 GHz and is connected to a Tektronix DPO2024B oscilloscope.

## Methods & Data

Before taking data, the cavity alignment and the iris present were adjusted to ensure that the laser is in the TEM-00 mode, as the derived equations depend on this alignment. LabVIEW was used to program the movement of the stepper motor, record the position of the stepper



motor, record the beat frequency from the spectrum analyzer at each step, and record the two modes of the cavity from the oscilloscope.

The following two sections break apart the two main values measured in this experiment—cavity length ( $\Delta L$ ) and beat frequency ( $f_b$ ). The breakdown includes how error was determined, values obtained, and how outliers were determined and removed. It also details how frequency pulling and pushing were minimized and how they effected the experiment. These two values were then plotted, and a linear fit was applied—this is detailed in the analysis.

## A) Cavity Length

Referring to Figure 2, most of the laser is enclosed with various indexes of refraction and lengths of each part of the laser. Thus, as stated in theory, the values in  $\frac{2(L_g n_g + L_m n_m + L_0 n_a)}{c}$  cannot be accurately measured. Because of the nature of the equation—its linearity—this value is an arbitrary starting point and is the intercept found by the fit. Thus, the cavity length,  $\Delta L$ , was the only value measured on the right-hand side of the following equation.

$$\frac{1}{f_b} = \frac{2\Delta L}{v_a} + \frac{2(L_g n_g + L_m n_m + L_0 n_a)}{c}$$

The stepper motor described in the experimental setup determines the  $\Delta L$  value. The stepper motor has a minimum distance it can move which is determined by the properties of the device. This minimum distance is referred to as 1 step. The step value measurement was done by taking 29 measurements of 1 step with error, arriving to a value of:

$$(2.50 \pm 0.08) * 10^{-6} \text{meters/step}$$

This step stated above is the value for the minimum distance the stage can move. However, a single step is not large enough to significantly effect the beat frequency. For this experiment,

data was taken every 20 steps. Thus, multiplying the value above by 20 and propagating error the distance for 20 steps is:

$$(5.00 \pm 0.16) * 10^{-5} \text{meters}$$

Taking data every 20 steps led us to taking a measurement for  $\Delta L$  at step values 20 steps, 40 steps, 60 steps, and so on. Assuming error is the same for every 20 steps, values for  $\Delta L$  were started at  $5.00 * 10^{-5} \text{meters}$  adding  $5.00 * 10^{-5} \text{meters}$  every time the motor moved. Error for each of these values was assumed uniform at  $\pm 0.16 * 10^{-5} \text{meters}$ .

The stepper motor was moved a total of 200 times leading to a total range from 0 meters to 0.01 meters for  $\Delta L$ . As discussed in the coming sections, the error for each  $\Delta L$  value (on the x-axis) was propagated into the beat frequency error (y-axis) in order to be factored into the linear fit.

## B) Frequency

The beat frequencies measured ranged from  $4.000 * 10^8 \text{ Hz}$  to  $4.756 * 10^8 \text{ Hz}$ . As stated earlier, the stepper motor moved 200 unique steps resulting in 200  $\Delta L$  values. At each of these  $\Delta L$  values, 20 beat frequency measurements ( $f_b$ ) were taken. First, meaningless data was removed.

Meaningless data for this experiment refer to beat frequencies of non-TEM-00 modes. These were removed because our equations used assume a TEM-00 lasing mode. Other meaningless data removed includes beat frequency data where the longitudinal modes were not at equal intensities. When the longitudinal modes are not at equal intensities, this means frequency pulling is occurring and thus changes the refractive index for each mode. These were removed because our equations assume the refractive index is uniform and identical for both longitudinal modes.

Beat frequencies less than  $4.0 \times 10^8 \text{ Hz}$  occur when the TEM-00 mode is not present and other modes are interfering. Thus, the beat frequencies that were measured to be less than  $4.0 \times 10^8 \text{ Hz}$  were removed. Again, this was done because our equations assume a TEM-00 lasing mode.

Frequency pulling is indicated by longitudinal modes not at equal intensities. In order to not exclude all data points, a tolerance was implemented. For this set of data, longitudinal modes that were more than 0.3 Volts apart were removed. 0.3 Volts was chosen because decreasing this value further removed a significant number of data points. A typical longitudinal mode had an intensity of about 0.8 Volts. These data points can be seen in Figure 5 on the right-hand side plot.

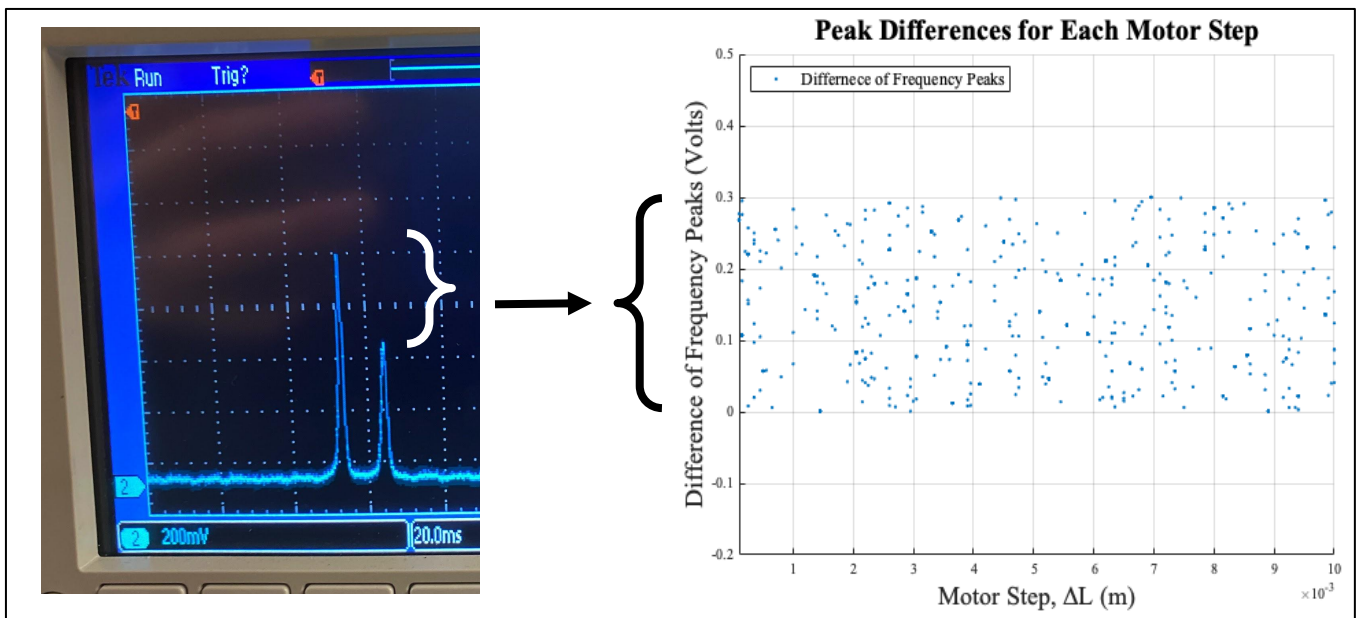


Figure 5: A Diagram showing the physical representation of the peak tolerance, and the corresponding values within the data set. The left-hand side is a typical output from the SFPI, showing the two longitudinal modes. The right-hand side is the corresponding values from the data, this shows an even spread and no pattern and minimizes frequency pulling.

After these two filtering techniques were implemented, a few beat frequency values were left at each  $\Delta L$ . The average beat frequency at each  $\Delta L$  and the error on the frequency were determined by using inverse-variance weighting.

Along with the error derived from the inverse-variance method, the error on  $\Delta L$  was propagated and added to the beat frequency error. After initial analysis showed the error was underestimated the error for each inverse beat frequency was multiplied by 20 before applying the linear fit:

$$\sigma_{f_b \text{ final}} = (\sigma_{f_b \text{ from weighed average}} + \text{propogated } \sigma \Delta L) * 20$$

The inverse beat frequency plotted against its cavity length is analyzed in the following section.

## Analysis & Results

Figure 6 depicts the plot of the inverse beat frequencies against the cavity lengths.

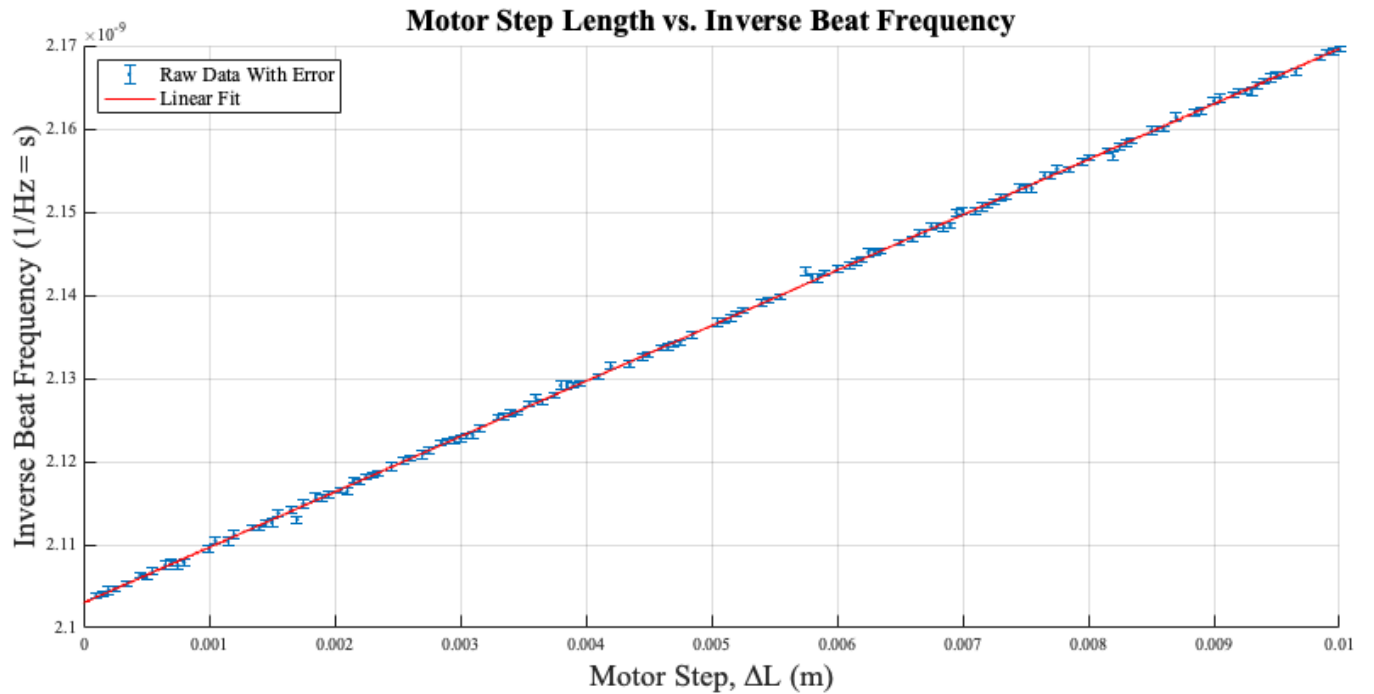


Figure 6: The plot of the 139 data points with their respective error. Error on  $\Delta L$  was propagated into the error of  $\sigma_{f_b}$ . The red line represents the linear fit on the data using the least squares algorithm provided by the advisors of the class. Resulting in a slope of  $(6.6625 \pm 0.0074) * 10^{-9}$  from the fit.

This set of data has 139 unique  $\Delta L$  values along with the respective inverse beat frequency after filtering. As is noted by the red line, a linear fit was applied to this plot. This fit was calculated by using the MATLAB *fit* function along with code provided by the advisors of this class (this can be found in Appendix A). The fitting algorithm uses a least squares algorithm to fit the weighted data to the linear model. This produced the following value for the slope of the line:

$$\text{slope} = (6.6625 \pm 0.0074) * 10^{-9}$$

Taking 2 over this value and propagating the error, the value for  $c$ , the speed of light in air, was measured to be:

$$c = (3.0019 \pm 0.0034) * 10^8 \text{ m/s}$$

Figure 7 is the weighted residual plot for each motor step. This results in a p-value of 0.99, a reduced Chi squared value of 0.609, and 137 degrees of freedom.

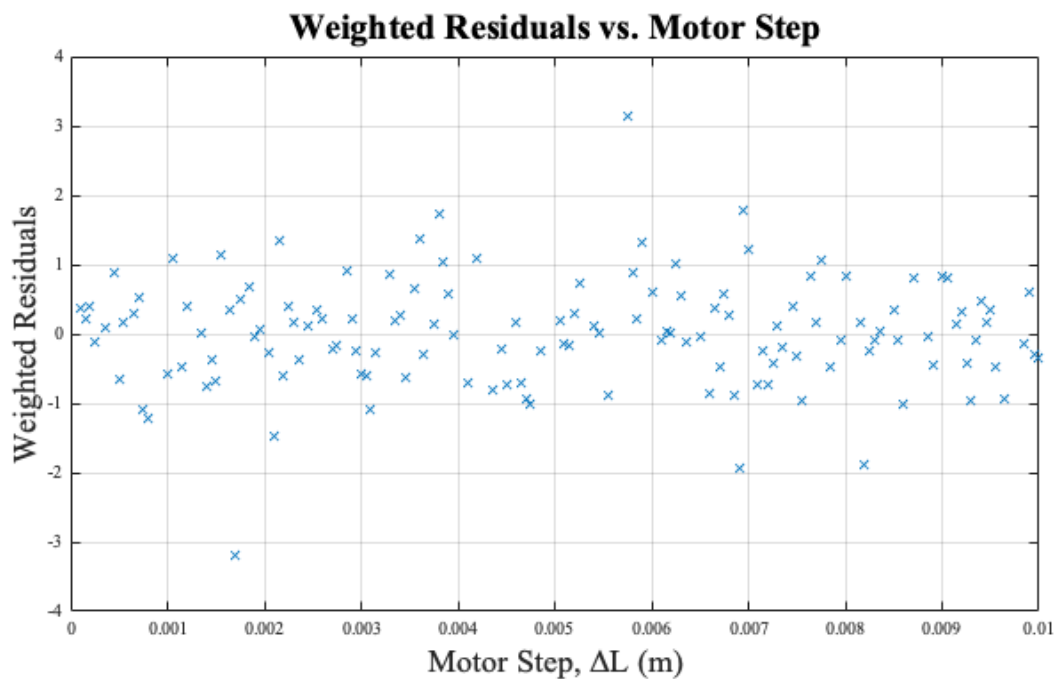


Figure 7: The plot of the 139 data points with their respective residual. The Chi squared value was calculated to be 0.609. The p-value was calculated to be 0.99. This plot was generated using part of the algorithm in Appendix A.

As mentioned above, frequency pulling was minimized by filtering the data before analysis. The other effect, frequency pushing has not been factored in yet. The following figure shows how the total intensity - the sum of the longitudinal modes for each beat frequency - changes as the laser cavity increases. Because of Covid-19 circumstances, further data on this effect was not able to be recorded.

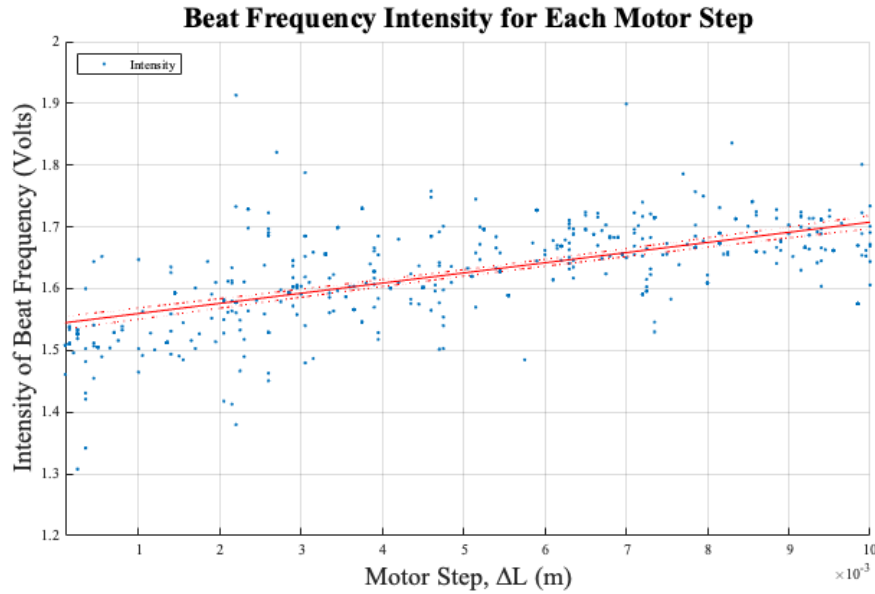


Figure 8: A plot of total intensity- the sum of each longitudinal mode peak for each beat frequency- as the cavity,  $\Delta L$ , increases. The plot includes 139 unique cavity lengths but includes multiple intensities from each cavity length. A linear fit was applied to this data calculating a slope of 1.83. From  $\Delta L = 0$  m to  $\Delta L = 0.001$  m, the intensity increases by about 10%.

In previous experiments<sup>4</sup> a change in total intensity of 10% lead to a  $\sim 9000$  Hz change in beat frequency. In our data, the total beat frequency intensity varied about 10% from the initial  $\Delta L$  value to the final  $\Delta L$  value. When beat frequencies range from  $4.0 \times 10^8$  Hz to  $4.756 \times 10^8$  Hz, the small effect of the 9000 Hz variation was omitted in the speed of light analysis. If further time permitted, this could have been factored into the experiment if the exact relationship of total intensity vs. beat frequency for our setup could have been quantified.

## Conclusion

In conclusion, by applying a linear regression, this method of calculating the speed of light produced a value of  $(3.0019 \pm 0.0034) * 10^8 \text{ m/s}$  for the speed of light in air. The uncertainty of  $0.0034 * 10^8 \text{ m/s}$  is not small enough to discriminate between the speed of light in air and the speed of light in a vacuum. This value for the speed of light has a percent difference of 0.13% from the accepted value of 299,792,458 m/s for the speed of light in air.

Effects of frequency pulling were included in analysis, however, due to time constraints, effects of frequency pushing were not incorporated into the analysis. Pushing is predicted to affect the beat frequencies up to about 10,000 Hz of variation for the larger cavity lengths based on previous experiments<sup>4</sup>. For comparison, a typical beat frequency was recorded in a range of 400,000,000 Hz to 475,600,000 Hz.

## Works Cited

- CPGM. (1983). Resolution 1 of the 17th CPM. *Bureau International des Poids et Mesures*. Retrieved from <https://www.bipm.org/en/CGPM/db/17/1/>, accessed 9-29-2020.
- Romer, M. (1676). A demonstration concerning the Motion of Light, communicated from Paris, in the Journal des Scavans, and here made English. *Philosophical Transactions*. Retrieved from <https://royalsocietypublishing.org/doi/10.1098/rstl.1677.0024>, accessed 9-29-2020.
- Brickner, R. G.; Kappers, L. A.; Lipschultz, F. P.; (1979). Determination of the speed of light by measurement of the beat frequency of internal laser modes, *American Journal of Physics* 47, 1086-7. doi:10.1119/1.11980.
- D'Orazio, D. J.; Pearson, M. J.; Schultz, J. T.; Sidor, D.; Best, M. W.; Goodfellow, K. M.; Scholten, R. E.; and White, J. D. (2010) Measuring the speed of light using beating longitudinal modes in an open-cavity HeNe laser, *American Journal of Physics* 78(5), 524-8. doi:10.1119/1.3299281.
- Javan, A.; Bennet, W. R.; and Herriott, D.R. (1960) Population inversion and continuous optical MASER oscillation in a gas discharge containing a He-Ne mixture, *Physical Review Letters* 6(3), 106-110. Retrieved from <https://journals.aps.org/prl/pdf/10.1103/PhysRevLett.6.106>, accessed 10-10-2020.
- Wang, C. P.; Varwig, R. L. (1979) Competition of Longitudinal and Transverse Modes in a CW HF Chemical Laser, *The Aerospace Corporation/DARPA*. Retrieved from <https://apps.dtic.mil/dtic/tr/fulltext/u2/a080382.pdf>, accessed 10/12/2020.
- Lindberg, Å. S. (1999). Mode frequency pulling in He-Ne lasers, *American Journal of Physics* 67(4), 350-3. Retrieved from <https://aapt-scitation-org.ezpl.lib.umn.edu/doi/pdf/10.1119/1.19261>, accessed 10/12/2020



# Appendix

## Appendix A: Matlab Code for Linear Fit and Chi Squared

```
% set values
x = TS_Locs_Plot;
y = Inv_Beat_freq_plot;
sig_y = Inv_Beat_freq_unc * 40;

%use a least squares algorithm to fit the weighted data to a model
[fitobj, gof, outp] = fit(x, y, 'poly1', 'Weights', (1./sig_y).^2)

%plot the original data vs. the selected model
figure
hold on
errorbar(x, y, sig_y, 'r', 'LineWidth', 0.1)
plot(fitobj, 'predfunc') % add another argument to change the default .95 conf. level
title('Motor Step Length vs. Inverse Beat Frequency, 95% Prediction Bounds');
xlabel('Motor Step, ΔL (m)', 'FontSize', 18)
ylabel('Inverse Beat Frequency (1/Hz = s)', 'FontSize', 18)
legend('Linear Fit', 'Prediction Bound', 'Prediction Bound', 'Raw Data With Error', 'Location', 'northwest')
grid on;
hold off

% Plot the weighted residuals (residuals divided by their standard deviation)
plot(x(1:length(outp.residuals)), outp.residuals, 'x')
title('Weighted Residuals vs. Motor Step, ΔL (m)')
xlabel('Motor Step, ΔL (m)')
ylabel('Weighted Residuals')
grid on

fprintf('Reduced Chi Squared: %E\n', gof.sse/gof.dfe);

% probability to exceed
pte = 1-chi2cdf(gof.sse, gof.dfe);
fprintf('PTE for SSE: %E and DFE: %E is: %E\n', gof.sse, gof.dfe, pte)

% Determine the uncertainty in the fit parameters (one sigma standard deviation)
mycoeffnames = coeffnames(fitobj); %get the fit coefficient names
mycoeffvalues = coeffvalues(fitobj); %get the fit coefficient values
mycoeff_onesig = diff(confint(fitobj))/4; %quick and dirty way to calculate the uncertainty by using the 95% confidence interval
error_matrix = inv(outp.Jacobian'*outp.Jacobian); %determine the uncertainty by using the Jacobian of the fit
dcov = diag(error_matrix); % (see "Measurements and their Uncertainties," Hughes and Hase, section 7.2, p.92.)
unc = sqrt(dcov); %Uncertainty in the fit parameters (Jacobian Method)
disp('Fit Parameters and Uncertainties (+/- One Standard Deviation)')
for irow = 1:outp.numparam
    % fprintf('%s: %E +/- %E\n', char( mycoeffnames(irow)), mycoeffvalues(irow), mycoeff_onesig(irow)) %quick and dirty method
    fprintf('%s: %E +/- %E\n', char( mycoeffnames(irow)), mycoeffvalues(irow), unc(irow)) %Jacobian Method
end
disp('Covariance or Error Matrix:')
error_matrix
disp('Correlation Matrix: ')
corrmat = error_matrix./sqrt(dcov*dcov)

C = 2./mycoeffvalues(1)
C_err = 2*unc(1)/(mycoeffvalues(1))^2
```